# New data on net-veined complexes in the Oslo Rift, southeastern Norway

TOM ANDERSEN, VIORICA MOROGAN & HENNING SØRENSEN

Andersen, T., Morogan, V. & Sørensen, H. 2004: New data on net-veined complexes in the Oslo Rift, southeastern Norway. *Norges geologiske undersøkelse Bulletin 442*, 29–38.

Bodies of basaltic trachyandesite occur in the endocontact zone of the Mykle granite against the large Skrim larvikite massif in the southern part of the Oslo igneous province.
New Sr and Nd isotope data indicate that the $^{87}Sr/^{86}Sr$ (0.704023-0.70544) and $\varepsilon_{Nd}$ (0.7-2.8) at 272 Ma of the basaltic trachyandesite are within the corresponding ranges of larvikite and the Vestfold basalts, but different from the Skien basalts. The isotopic data support a model for the origin of the trachyandesite by mixing of basic and granitic or syenitic melts, which is also in accordance with trace element data and petrographic observations. Black and emulsified trachyandesites have uniform $\varepsilon_{Nd}$ (+2.2 ± 0.5), but variable $^{87}Sr/^{86}Sr$, which indicate that the melts were heterogeneous in Sr isotopes at the time of emplacement, most probably because of selective introduction of radiogenic Sr from older rocks by a fluid phase before or during emplacement. Globular bodies of granite in the basaltic trachyandesite are surrounded by biotite haloes in the trachyandesite and are thought to be lumps of partially consolidated granite or of the already consolidated granite picked up by the hot trachyandesitic magma.

*Tom Andersen, Institutt for geofag, Universitetet i Oslo, Postboks 1047 Blindern, N-0316 Oslo, Norge. Viorica Morogan, Rörstrandsgatan 19, 4 tr., S-11340 Stockholm, Sverige. Henning Sørensen, Geologisk Institut, Øster Voldgade 10, DK-1350 København K, Danmark.*

## Introduction

Net-veined complexes composed of globular masses of fine-grained basic igneous rocks and veins of coarser grained syenitic and granitic rocks were described from the Late Palaeozoic Oslo Rift by Morogan & Sørensen (1994). The net-veined complexes occur in the area around Lake Mykle in the southwestern part of the Rift, where they are located in the complicated contact zone of a body of granite which intrudes into plutonic masses of larvikite (Bonin & Sørensen 2003).

The results of Morogan & Sørensen (1994) indicate that magma of basaltic trachyandesite (for simplicity hereafter called trachyandesite) were emplaced into a granitic-syenitic magma chamber and rose along the walls of the chamber in a zone of weakness between a marginal shell of already consolidated granite and the main mass of still at least partially fluid granitic magma. The trachyandesite formed sheets along the walls which were invaded by several generations of veins of syenite and granite (Morogan & Sørensen 1994, fig. 19).

In the present paper, new information on the net-veined complexes of the Mykle area are reported: (1) Sr- and Nd-isotope data on most of the trachyandesites analysed by Morogan & Sørensen (1994) and on some associated granites; (2) description of an emulsified type of basic enclaves in acidic rocks; and (3) ellipsoidal bodies of granite enclosed in the main mass of trachyandesite.

## Field relationships and petrography

Morogan & Sørensen (1994) distinguished three types of basaltic trachyandesite: *grey, black* and *hybrid*. The grey type is slightly more coarse-grained than the black type. Three stages of crystallization were observed in the black type: 1. Macrocrysts of plagioclase and clinopyroxene; 2. Granular amphibole, biotite, clinopyroxene, feldspar, iron-titanium oxides, apatite and titanite; some quartz was also formed in the grey rock at this stage. 3. A dense matrix of feldspar, clinopyroxene, amphibole, biotite, titanite and a multitude of apatite needles and skeletal crystals of iron-titanium oxides. Only stages 1 and 2 are present in the grey type. Xenocrysts of clinopyroxene and plagioclase indicate that the basaltic trachyandesitic magmas were formed by mixing of basaltic and trachytic magmas. Trachyandesites containing grains of quartz and potassium feldspar represent the hybrid type distinguished by Morogan & Sørensen (1994). (We use the term 'macrocryst' as a general, non-genetic term for phenocrysts and xenocrysts. Xenocrysts are distinguished by their morphology, reaction rims and chemical composition.)

### Emulsified type of basic enclaves in granite

At Sørmyr to the northwest of Lake Mykle (Fig. 1), the contact between the Mykle granite body and the large Skrim massif of larvikite to the north is sharp and well exposed. The medium-grained reddish granite of the contact zone is 30 m wide and without any traces of basic enclaves. To the south it borders on a sheet of trachyandesite which is a massive, fine-grained to aphanitic, grey and black rock intersected by several generations of veins of syenite and granite. The youngest of these is coarse-grained and identical to the ekerite (peralkaline granite) which forms the major part of the Mykle granite body (Bonin & Sørensen 2003, fig. 4). The homogeneous trachyandesite passes, after a few metres, into a mottled rock composed of grey to black rounded

globules enclosed in a matrix which appears to be a mixture of trachyandesite and granite (Fig. 2). The globules vary in size from a few millimetres to several centimetres. The largest are of a more dense, black colour than the smaller ones (Fig. 2). This mélange of basic globules and more felsic matrix recalls the emulsified type of basic enclaves in acid rocks described by Gourgaud (1991). The transition from the emulsified rock to the main mass of granite to the south is unexposed.

The massive trachyandesite (101252) is of the black type distinguished by Morogan & Sørensen (1994). It is composed of amphibole, biotite, plagioclase, titanite, apatite needles and crystals as well as skeletal crystal of Fe-Ti oxides. The amphibole is partly overgrown by biotite. Patches of chlorite most probably represent altered clinopyroxene. Quartz was not observed.

The emulsified rock (101253) is a mélange of trachyandesite and a network of veins and nests of quartz and turbid perthitic potassium feldspar. The grain size of quartz and K-feldspar is similar to or larger than that of the trachyandesite. It should be noted that there is no concentration of biotite in the felsic parts of the emulsified rock and that the trachyandesite does not appear to have been modified during the mingling of basic and acid material. It is, however, distinguished from the trachyandesite to the north of the emulsified rock by the presence of scattered grains of quartz.

## Ellipsoidal bodies of granite in trachyandesite

The massive trachyandesite at Sørmyr contains scattered ellipsoidal 'globules' of coarse-grained granite measuring up to about 20 cm along their long axes (Figs. 3, 4). Two granite globules appear to coalesce and partially overlap (Fig. 4). There is a concentration of biotite in the contact zone between granite and trachyandesite which is difficult to see on fresh surfaces (Fig. 3) but very distinct on weathered surfaces (Fig. 4).

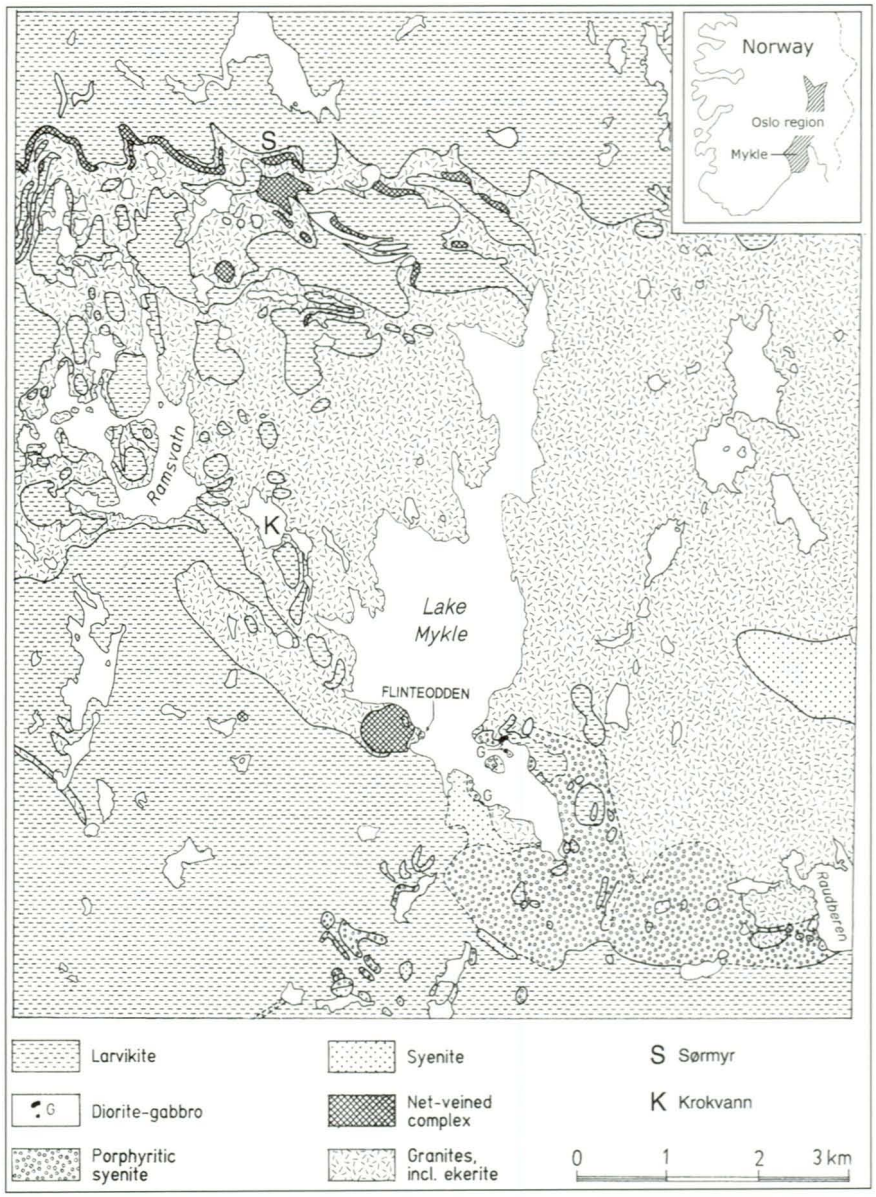


Fig. 1. Simplified geological map of the Mykle region.

Fig. 2. Emulsified trachyandesite with interstitial granite. Note the black dots of denser black colour in the upper and lower parts of the photograph. Sørmyr to the northwest of lake Mykle. (Hammer head 17 cm long).

Fig 3. Granite globule in trachyandesite; Sørmyr. The globule is 15 cm in length. The light-coloured surface above the hammer head is discolouration of a fracture surface.

The regional granite (101268) is coarsegrained and composed of quartz and turbid perthite. It contains scattered grains of plagioclase. There are small grains of biotite, zircon and opaque minerals and aggregates of rusty material which, from other exposures, are known to be alteration products of pyroxene and/or amphibole. This rock belongs to the fine- to medium-grained reddish granites distinguished by Bonin & Sørensen (2003).

The granite of the globules (92064, 101254, 101269) is coarsegrained and dominated by quartz and perthite, in part in micrographic intergrowths, and contains scattered small grains of brown biotite but also, in places, small grains of green to bluish amphibole. There are aggregates of amphibole, biotite, titanite, opaque minerals and apatite which are interpreted to be enclaves of trachyandesite. In the contact against the enclosing trachyandesite there is a concentration of biotite which, together with some quartz, impregnates the trachyandesite. It should be noted that there appears to be no K-feldspar present in the trachyandesite.

## Mineral chemistry

The chemical composition of the main minerals was analysed with a JEOL 733 electron microprobe equipped with a TRACOR energy-dispersive system at the Geological Institute, University of Copenhagen. The pyroxenes were classified after Morimoto et al. (1988) and the amphiboles after Leake et al. (1997).

### Homogeneous trachyandesite and emulsified basic enclaves

The main mafic phase in the homogeneous basaltic trachyandesite (101252) is biotite with a high Ti content and a low Si content (Table 1, no. 2). The amphiboles belong to the calcic group (CaB >1.5) and display a common magmatic to sub-magmatic trend of crystallization from magnesio-hornblende to actinolite and also edenite (Table 2, nos. 1, 2, 3), similar to the amphibole analyses of Morogan & Sørensen (1994).

The emulsified basaltic trachyandesite (101253 c) contains small grains of a greenish pyroxene classified as an aluminian (Al >0.1) and sodian (Na >0.1) augite (Table 3, nos. 1, 2). This augite contains only 26 % Wo, very close to a subcalcic augite composition which involves Ac (Na-Fe3+), Jd(Na-Alvi) and Al-Ts (Alvi-Aliv) substitutions. It should be noted that similar pyroxenes occur in the groundmass of the tra-

Fig. 4. Coalescing granite globules in trachyandesite which is enriched in biotite adjacent to the granite. The weathered trachyandesite is white. Sørmyr.

Table 1. Representative compositions of biotite.

| | 1 | 2 | 3 | 4 | 5 | 6 |
|---|---|---|---|---|---|---|
| **Sample** | **101252** | | **101254** | | **101269** | **92064** |
| **Rock type*** | **h.b.tra** | | **b.tra** | | **b.tra/gt** | **gt/b.tra** |
| $SiO_2$ | 37.12 | 36.29 | 37.89 | 36.97 | 39.14 | 39.10 |
| $TiO_2$ | 2.84 | 3.90 | 3.66 | 3.58 | 2.79 | 2.81 |
| $Al_2O_3$ | 11.83 | 11.80 | 12.18 | 12.42 | 11.38 | 10.98 |
| FeO | 25.64 | 25.76 | 19.26 | 21.75 | 20.55 | 22.22 |
| MnO | 0.41 | 0.19 | 0.18 | 0.13 | 0.42 | 0.32 |
| MgO | 9.01 | 8.02 | 12.07 | 11.14 | 11.82 | 11.05 |
| CaO | 0.23 | 0.00 | 0.09 | 0.16 | 0.00 | 0.08 |
| $Na_2O$ | 0.15 | 0.00 | 0.06 | 0.09 | 0.10 | 0.09 |
| $K_2O$ | 8.80 | 9.66 | 9.97 | 9.99 | 9.85 | 9.81 |
| Total | 96.03 | 95.62 | 95.36 | 96.23 | 96.05 | 96.46 |
| | | | Cations (O = 22) | | | |
| Si | 5.806 | 5.739 | 5.806 | 5.695 | 5.974 | 5.991 |
| Ti | 0.334 | 0.464 | 0.422 | 0.415 | 0.320 | 0.324 |
| Al | 2.181 | 2.199 | 2.200 | 2.255 | 2.047 | 1.983 |
| $Fe^{2+}$ | 3.354 | 3.407 | 2.468 | 2.802 | 2.623 | 2.847 |
| Mn | 0.054 | 0.025 | 0.023 | 0.017 | 0.054 | 0.042 |
| Mg | 2.101 | 1.890 | 2.757 | 2.558 | 2.689 | 2.523 |
| Ca | 0.039 | 0.000 | 0.015 | 0.026 | 0.000 | 0.013 |
| Na | 0.045 | 0.000 | 0.018 | 0.027 | 0.030 | 0.027 |
| K | 1.756 | 1.949 | 1.949 | 1.963 | 1.918 | 1.917 |
| XMg | 0.39 | 0.36 | 0.53 | 0.48 | 0.51 | 0.47 |

*see Table 3 for abbreviations

Table 2. Representative amphibole compositions.

| | 1 | 2 | 3 | 4 | 5 | 6 | 7 | 8 | 9 | 10 |
|---|---|---|---|---|---|---|---|---|---|---|
| **Sample** | **101252** | | | **101269** | | | | **92064** | | |
| **Rock type*** | **h.b.tra** | | | **gt/b.tra** | | | | **gt/b.tra** | | |
| **Name**** | **ed** | **act** | **Mhb** | **Marvf** | **Mrieb** | **ed** | **Mhb** | **Mhb** | **ed** | **Mhb** |
| $SiO_2$ | 49.66 | 51.66 | 50.31 | 53.32 | 54.52 | 49.10 | 50.78 | 51.03 | 49.26 | 49.02 |
| $TiO_2$ | 1.00 | 0.58 | 0.77 | 1.43 | 0.67 | 0.80 | 0.70 | 0.59 | 1.13 | 0.91 |
| $Al_2O_3$ | 4.67 | 2.77 | 3.38 | 0.42 | 0.50 | 4.69 | 3.81 | 3.23 | 4.63 | 4.06 |
| FeO | 15.46 | 15.70 | 16.45 | 19.21 | 22.91 | 16.76 | 14.51 | 15.49 | 16.04 | 14.98 |
| MnO | 0.30 | 0.53 | 0.27 | 0.14 | 0.29 | 0.37 | 0.54 | 0.46 | 0.47 | 0.65 |
| MgO | 13.91 | 13.39 | 12.89 | 9.73 | 7.99 | 12.65 | 14.26 | 14.07 | 12.97 | 13.27 |
| CaO | 10.77 | 10.64 | 11.19 | 0.54 | 0.96 | 10.82 | 10.81 | 10.84 | 11.02 | 10.66 |
| $Na_2O$ | 2.24 | 1.77 | 1.71 | 8.14 | 7.35 | 2.33 | 1.70 | 1.80 | 2.35 | 2.04 |
| $K_2O$ | 0.45 | 0.21 | 0.36 | 1.08 | 0.91 | 0.58 | 0.39 | 0.41 | 0.64 | 0.52 |
| Total | 98.46 | 97.25 | 97.33 | 94.01 | 96.10 | 98.10 | 97.50 | 97.92 | 98.51 | 96.11 |
| | | | | Cations (O=23) | | | | | | |
| Si | 7.275 | 7.623 | 7.474 | 8.210 | 8.305 | 7.281 | 7.455 | 7.495 | 7.261 | 7.361 |
| AlIV | 0.725 | 0.377 | 0.526 | 0.000 | 0.000 | 0.719 | 0.545 | 0.505 | 0.739 | 0.639 |
| Ti | 0.110 | 0.064 | 0.086 | 0.166 | 0.077 | 0.089 | 0.077 | 0.065 | 0.125 | 0.103 |
| AlVI | 0.081 | 0.105 | 0.066 | 0.076 | 0.090 | 0.101 | 0.114 | 0.054 | 0.065 | 0.080 |
| $Fe^{2+}$ | 1.894 | 1.937 | 2.044 | 0.866 | 1.699 | 2.078 | 1.781 | 1.903 | 1.977 | 1.651 |
| Mn | 0.037 | 0.066 | 0.034 | 0.018 | 0.037 | 0.046 | 0.067 | 0.057 | 0.059 | 0.083 |
| Mg | 3.037 | 2.945 | 2.584 | 2.233 | 1.814 | 2.796 | 3.120 | 3.080 | 2.849 | 2.970 |
| Ca | 1.691 | 1.682 | 1.781 | 0.089 | 0.157 | 1.719 | 1.700 | 1.706 | 1.740 | 1.715 |
| Na | 0.363 | 0.506 | 0.493 | 2.430 | 2.171 | 0.670 | 0.484 | 0.513 | 0.672 | 0.594 |
| K | 0.084 | 0.040 | 0.068 | 0.212 | 0.177 | 0.110 | 0.073 | 0.077 | 0.0120 | 0.100 |
| CaB | 1.691 | 1.682 | 1.781 | 0.056 | 0.094 | 1.719 | 1.700 | 1.706 | 1.740 | 1.715 |
| NaB | 0.149 | 0.202 | 0.136 | 1.944 | 1.906 | 0.071 | 0.141 | 0.138 | 0.487 | 0.309 |
| (Na+K)A | 0.571 | 0.344 | 0.425 | 0.698 | 0.442 | 0.70 | 0.416 | 0.452 | 0.607 | 0.409 |
| $Fe^{3+}$ | 0.000 | 0.000 | 0.000 | 1.608 | 1.220 | 0.000 | 0.000 | 0.000 | 0.000 | 0.230 |
| Mg/Mg+Fe | 0.61 | 0.60 | 0.58 | 0.72 | 0.52 | 0.57 | 0.64 | 0.62 | 0.59 | 0.64 |

*h.b.tra = homogeneous basaltic trachyandesite; b.tra = basaltic trachyandesite; gt = granite
**ed = edenite; act = actinolite; Mhb = magnesio-hornblende; Marf = magesino-arvedsonite; Mrieb = magnesio-riebeckite

chyandesite hosting granitic ellipsoidal bodies (Table 3, nos. 3, 7).

### Ellipsoidal granitic bodies in trachyandesite

The mineral chemistry of the basaltic trachyandesite (92064, 101254, 10269) hosting the granite globules (92064,101269) was found to be very similar to that of the rocks described by Morogan & Sørensen (1994). Three pyroxene types were identified: aluminian diopside macrocrysts (Table 3, nos. 5, 6), diopside phenocrysts (Table 3, no. 4) and small groundmass grains of aluminian and sodian augite (Table 3, nos. 3, 7). The biotite of the trachyandesite shows fairly high Ti and low Si contents (Table 1, nos. 5, 6), relative to the biotite of the contact zone between trachyandesite and granite ellipsoids (Table 1, nos. 3 and 4) which exhibits compositions more similar to those of the granite.

At the contact with the granite ellipsoids, the trachyandesite contains very few augite grains (Table 3, no. 7) surrounded by biotite. Calcic amphiboles, magnesio-hornblende (Table 2, no. 7) and edenite (Table 2, no. 6) are the main mafic minerals in the trachyandesite enclosing the granite ellipsoids. The granite ellipsoids contain sodic amphiboles (NaB >1.5) such as magnesio-arfvedsonite and magnesio-riebeckite (Table 2, nos. 4, 5). The Fe-Ti oxides of trachyandesite and granite ellipsoids (Table 4) show extensive re-equilibration.

## Whole-rock major and trace element chemistry

Four samples were selected for chemical analyses: 101252 represents the homogeneous sheet of trachyandesite; 101253c is a single black globular body about 5 cm in diameter from the emulsified type of rock; 101253a is a collection of dark globules from the emulsified rock handpicked from the mixed rock; and 101253b is the whole emulsified rock composed of basic and acid parts. The results are presented in Table 5 together with the ranges in chemical composition of the various types of trachyandesite from net-veined complexes examined by Morogan & Sørensen (1994).

The chemical composition of the homogeneous massive trachyandesite from Sørmyr falls within the range in composition indicated for the grey type of trachyandesite. The single black globule of basic rock and the collection of dark globules fall

Table 3. Representative compositions of pyroxene from Sørmyr.

| | 1 | 2 | 3 | 4 | 5 | 6 | 7 |
|---|---|---|---|---|---|---|---|
| **Sample** | **101252** | | **101254** | | | | **101269** |
| **Rock type*** | **h.b.tra** | | **b.tra** | | | | **b.tra/gt** |
| $SiO_2$ | 50.61 | 50.90 | 54.99 | 51.23 | 50.62 | 48.79 | 53.71 |
| $TiO_2$ | 1.11 | 1.10 | 0.16 | 0.53 | 1.03 | 2.11 | 0.27 |
| $Al_2O_3$ | 4.32 | 4.51 | 1.81 | 1.92 | 3.02 | 4.13 | 1.87 |
| FeO | 16.92 | 16.07 | 12.82 | 9.26 | 7.71 | 9.61 | 14.60 |
| MnO | 0.52 | 0.52 | 0.44 | 0.47 | 0.56 | 0.24 | 0.75 |
| MgO | 13.12 | 13.53 | 16.87 | 12.67 | 13.42 | 13.70 | 15.42 |
| CaO | 11.08 | 11.00 | 11.81 | 23.40 | 23.04 | 20.83 | 11.53 |
| $Na_2O$ | 1.77 | 1.76 | 0.79 | 0.40 | 0.54 | 0.57 | 1.49 |
| $K_2O$ | 0.46 | 0.53 | 0.19 | 0.08 | 0.05 | 0.00 | 0.00 |
| Total | 99.91 | 99.92 | 99.88 | 99.96 | 99.99 | 99.98 | 99.64 |
| | | | Cations (O= 6) | | | | |
| Si | 1.900 | 1.903 | 2.038 | 1.918 | 1.880 | 1.818 | 2.004 |
| Al IV | 0.100 | 0.097 | 0.000 | 0.082 | 0.120 | 0.182 | 0.000 |
| Ti | 0.031 | 0.031 | 0.004 | 0.015 | 0.029 | 0.059 | 0.008 |
| Ai VI | 0.091 | 0.102 | 0.079 | 0.003 | 0.012 | 0.000 | 0.082 |
| $Fe^{3+}$ | 0.098 | 0.085 | 0.000 | 0.083 | 0.091 | 0.105 | 0.002 |
| $Fe^{2+}$ | 0.433 | 0.417 | 0.498 | 0.207 | 0.149 | 0.195 | 0.454 |
| Mn | 0.017 | 0.016 | 0.014 | 0.015 | 0.018 | 0.008 | 0.024 |
| Mg | 0.734 | 0.754 | 0.932 | 0.707 | 0.743 | 0.761 | 0.858 |
| Ca | 0.446 | 0.441 | 0.469 | 0.938 | 0.917 | 0.832 | 0.461 |
| Na | 0.129 | 0.128 | 0.057 | 0.029 | 0.039 | 0.041 | 0.108 |
| K | 0.022 | 0.025 | 0.009 | 0.004 | 0.002 | 0.000 | 0.000 |
| Q | 1.6 | 1.6 | 1.8 | 1.9 | 1.9 | 1.9 | 1.9 |
| J | 0.3 | 0.3 | 0.2 | 0.1 | 0.1 | 0.1 | 0.2 |
| End members | | | | | | | |
| Wo | 26 | 26 | 26 | 48 | 48 | 44 | 26 |
| En | 42 | 44 | 48 | 36 | 39 | 40 | 47 |
| Fs | 32 | 30 | 16 | 16 | 13 | 16 | 27 |

* e.b.tra = emulsified basaltic trachyandesite; b.tra = basaltic trachyandesite; gt = granite

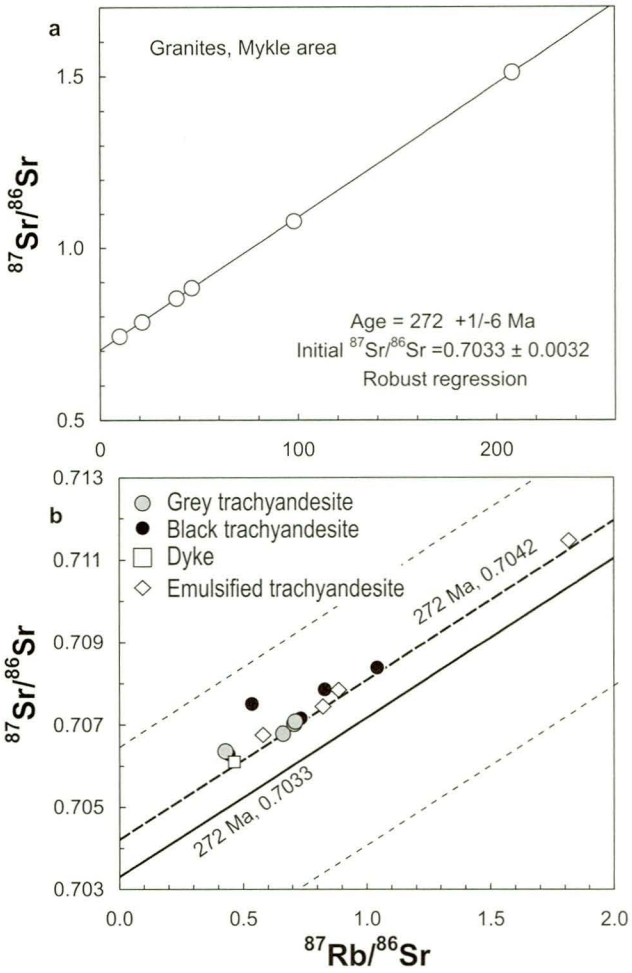


Fig. 6. Rb-Sr isochron diagram a: Granites. b: Basaltic trachyandesites, compared to the granite reference line (solid line) and its error envelope (broken lines).

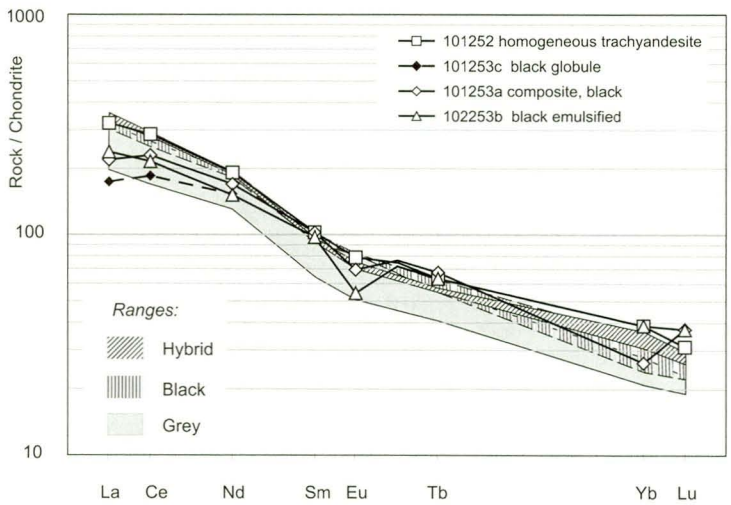


Fig. 5 Chondrite normalized REE diagrams. Chondritic values from Boynton (1984).

chemically between the homogeneous trachyandesite and the composition of the hybrid types analysed by Morogan & Sørensen (1994), whereas the mixture of basic and acid rocks (101253b) falls beyond the range indicated for the hybrid, but still homogeneous type of Morogan & Sørensen (1994). The single black globule (101253c) and the collection of dark globules (101253a) differ from the homogeneous trachyandesite (101252) in their distinctly higher $Na_2O$ and lower $K_2O$, Rb and Ba which indicates that they have a lower content of potassium feldspar. The single black globule also has lower contents of REE. In the chondrite-normalised REE diagram (Fig. 5), the homogeneous basic rock (101252) shows a strong enrichment in LREE relative to HREE and no Eu anomaly, as described by Morogan & Sørensen, 1994, fig. 13) for the grey and black trachyandesite. The emulsified rocks (101253 a and b) display weak Eu anomalies and an enrichment in the HREE, as also found by Morogan & Sørensen (1994) for the hybrid trachyandesite.

Table 4. Compositions of iron-titanium oxides.

| (A) Ilmenite | | | | (B) Magnetite | | | |
|---|---|---|---|---|---|---|---|
| | 1 | 2 | 3 | | 1 | 1 | 3 |
| Sample | 101254 | 101269 | 92064 | Sample | 101253 | 101269 | 92064 |
| Rock type | b.tra | b.tra/gt | gt/b.tra | Rock type | e.b.tra | b.tra/gt | gt/b.tra |
| $SiO_2$ | 0.23 | 0.42 | 0.26 | $SiO_2$ | 0.16 | 0.16 | 0.35 |
| $TiO_2$ | 50.01 | 50.01 | 50.30 | $TiO_2$ | 0.28 | 0.51 | 0.00 |
| $Al_2O_3$ | 0.00 | 0.17 | 0.00 | $Al_2O_3$ | 0.00 | 0.19 | 0.00 |
| $Cr_2O_3$ | 0.00 | 0.01 | 0.00 | $Cr_2O_3$ | 0.02 | 0.08 | 0.06 |
| FeO | 47.17 | 45.91 | 42.57 | FeO | 92.62 | 91.14 | 91.84 |
| MnO | 2.59 | 3.06 | 3.67 | MnO | 0.21 | 0.14 | 0.00 |
| NiO | 0.03 | 0.00 | 0.12 | NiO | 0.00 | 0.00 | 0.00 |
| MgO | 0.00 | 0.20 | 0.00 | MgO | 0.35 | 0.15 | 0.00 |
| Total | 100.03 | 99.78 | 96.92 | Total | 93.64 | 92.37 | 92.25 |
| | Cations (O= 2) | | | | Cations O = 3) | | |
| Si | 0.006 | 0.011 | 0.007 | Si | 0.006 | 0.006 | 0.014 |
| Ti | 0.946 | 0.946 | 0.984 | Ti | 0.008 | 0.015 | 0.000 |
| Al | 0.000 | 0.005 | 0.000 | Al | 0.000 | 0.000 | 0.082 |
| Cr | 0.000 | 0.000 | 0.000 | Cr | 0.001 | 0.002 | 0.002 |
| Fe | 0.992 | 0.966 | 0.926 | Fe | 2.959 | 2.955 | 2.985 |
| Mn | 0.055 | 0.065 | 0.081 | Mn | 0.007 | 0.005 | 0.000 |
| Ni | 0.001 | 0.000 | 0.003 | Ni | 0.000 | 0.000 | 0.000 |
| Mg | 0.000 | 0.007 | 0.000 | Mg | 0.020 | 0.009 | 0.000 |
| $Fe^{3+}$ | 0.096 | 0.082 | 0.019 | $Fe^{3+}$ | 1.971 | 1.947 | 1.971 |
| $Fe^{2+}$ | 0.896 | 0.884 | 0.907 | $Fe^{2+}$ | 0.987 | 1.008 | 1.014 |
| End members % | | | | End members % | | | |
| il | 95 | 96 | 99 | ulv | 2 | 5 | 0 |
| hm | 5 | 4 | 1 | mt | 98 | 95 | 100 |

## Rb-Sr and Sm-Nd isotope systematics

Rb, Sr, Sm and Nd concentrations in 10 samples of basaltic trachyandesite, and 6 samples of granite were determined by isotope dilution analysis, and Sr and Nd isotope ratios by thermal ionization mass spectrometry, using Finnigan MAT262 and VG 354 mass spectrometers in the Laboratory of Isotope Geology at the Mineralogical-Geological Museum, University of Oslo (Table 6). Chemical separation, spiking and analytical procedures were the same as used in Andersen et al. (2001). During the period of analysis, the NBS SRM 987 Sr isotope standard gave $^{87}Sr/^{86}Sr$ = 0.710190 ± 0.000050 (2σ, and the Johnson and Matthey batch No. S819093A $Nd_2O_3$ gave $^{143}Nd/^{144}Nd$ = 0.511101 ± 0.000013 (2σ). Samples 101252, 101253a, b, c, were analysed at the Geological Institute, University of Copenhagen, by methods described in Andersen et al. (2004). The mean value for the internal JM Nd standard (referenced against La Jolla) during the period of measurement was 0.511115 for $^{143}Nd/^{144}Nd$, with a 2σ external reproducibility of ± 0.000013 (five measurements). The mean $^{87}Sr/^{86}Sr$ value of the NBS 987 Sr standard was 0.710248 with a 2σ external reproducibility of 0.000011 (four measurements). Geochronological calculations were made using Isoplot/Ex 3.0 (Ludwig 2003).

The six samples of granite have low Sr concentrations (3-37 ppm), and high $^{87}Rb/^{86}Sr$ ratios (9.8-208), and define a poor (MSWD=43) correlation line with an age of 272 +1/-6 Ma and an initial $^{87}Sr/^{86}Sr$ ratio of 0.7033 ± 0.0032 (Fig. 6a), using the robust regression algorithm in Isoplot/Ex (Ludwig 2003). The age indicated by the regression line is indistinguishable from whole-rock Rb-Sr isochron ages of 270 ± 4 Ma for syenite from the Siljan area (Sundvoll & Larsen 1990) and 271 ± 2 Ma for ekerite from the Eikern pluton (Rasmussen et al. 1988). The initial $^{87}Sr/^{86}Sr$ ratios of those isochrons (0.7042±0.0003 and 0.7053 ± 0.0006, respectively) are also indistinguishable from the initial ratio of the present regression line, within its large uncertainty. The poor fit may be due to a heterogeneous initial Sr isotopic composition on the scale sampled here, or to a minor disturbance of some of the samples with very high Rb/Sr; the elevated Rb/Sr and low Sr concentration make these rocks susceptible to loss of radiogenic Sr during late-stage hydrothermal alteration and recent weathering.

The samples of grey, black and emulsified trachyandesite have higher Sr concentrations (133-781 ppm) and correspondingly low $^{87}Rb/^{86}Sr$ (= 1.82). All points plot above the regression line

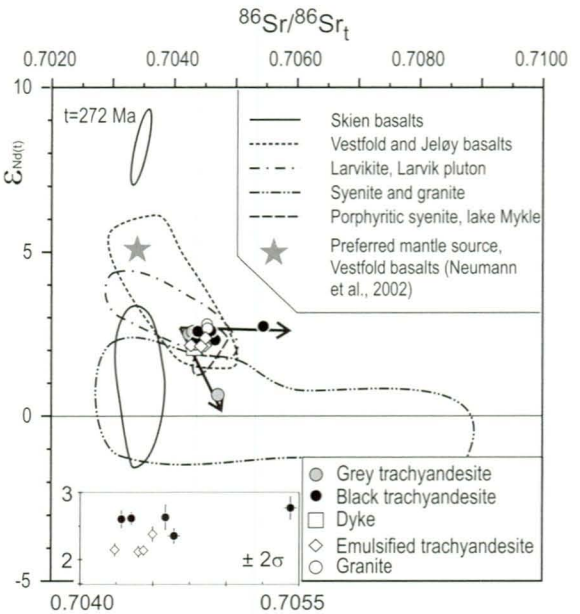


Fig. 7. Sr and Nd isotopic compositions at 272 Ma. The expanded detail in the lower left part of the diagram shows the compositions of black and emulsified trachyandesites at 272 Ma, with ±2σ error bars, where these exceed the symbol size (symbols as in the main part of the figure). Black arrows: Mixing trends illustrating hydrothermal (horizontal arrow) and bulk (sloping arrow) contamination trends of mantle-derived magma with old, crustal material. Sources of reference data: Skien basalts: Dunworth et al. (2001), Vestfold and Jeløy basalts: Neumann et al. (2002), Larvikite, syenite and granite: Neumann et al. 1988, Trønnes & Brandon (1992), Porphyritic syenite: Andersen et al. (2004). The dyke is a disrupted basic dyke described by Morogan & Sørensen (1994).

Table 5. Chemical analyses of trachyandesite sheet and emulsified type of enclaves from Sörmyr, NW of lake Mykle, the Oslo igneous province together with analyses quoted from Morogan & Sørensen (1994).

| | 101252 homogeneous sheet of trachyandesite | 101253c single black globule in emulsified trachyandesite | 101253a hand-picked concentrate of dark part of emulsified trachyandesite | 102253b total analysis of emulsified trachyandesite comprising basic and acid components | range in composition of grey type of trachyandesite[1)] | range in composition of black type of trachyandesite[1)] | range in composition of hybrid type of trachyandesite[1)] |
|---|---|---|---|---|---|---|---|
| | | | | Weight percent oxides | | | |
| $SiO_2$ | 51.29 | 54.33 | 54.95 | 58.13 | 50.6-52.1 | 51.9-52.1 | 55.0-56.3 |
| $TiO_2$ | 2.89 | 2.53 | 2.47 | 2.08 | 2.6-3.1 | 2.6-2.7 | 2.1-2.2 |
| $Al_2O_3$ | 14.19 | 14.19 | 14.32 | 13.86 | 14.2-14.6 | 14.5-14.8 | 14.7-15.0 |
| $Fe_2O_3$ | 3.23 | 3.13 | 3.38 | 3.45 | 0.8-3.2 | 1.1-2.2 | 1.8-2.6 |
| FeO | 7.30 | 6.43 | 5.82 | 4.46 | 7.3-9.2 | 7.3-8.5 | 5.7-5.9 |
| MnO | 0.23 | 0.22 | 0.22 | 0.24 | 0.2 | 0.2 | 0.2 |
| MgO | 3.51 | 3.23 | 3.01 | 2.47 | 3.3-4.2 | 3.3-3.4 | 2.5-2.7 |
| CaO | 5.48 | 4.89 | 4.85 | 4.12 | 5.4-6.5 | 5.6-5.9 | 4.2-4.5 |
| $Na_2O$ | 5.01 | 7.18 | 6.55 | 4.94 | 4.2-5.3 | 5.2-5.4 | 5.3-5.5 |
| $K_2O$ | 3.07 | 0.63 | 1.39 | 3.75 | 2.3-3.4 | 3.1-3.2 | 3.5-3.9 |
| $P_2O_5$ | 1.73 | 1.47 | 1.43 | 1.21 | 1.0-1.8 | 1.6 | 1.1-3.1 |
| loi | 1.25 | 0.81 | 0.86 | 0.70 | 1.6-2.3 | 1.3-1.5 | 1.5 |
| total | 99.18 | 99.04 | 99.25 | 99.42 | | | |
| | | | | CIPW norm | | | |
| *q* | 0 | 0 | 0.77 | 6.68 | 0 | 0 | 0-0.06 |
| *ne* | 0 | 0 | 0 | 0 | 0-0.65 | 2.08-2.89 | 0 |
| *hy* | 1.53 | 5.44 | 8.22 | 5.44 | 0.28-7.10 | 0 | 2.01-8.92 |
| | | | | Parts per million | | | |
| Sc | 19.2 | 17 | 16.5 | 14.6 | 18.0-19.7 | 17.9-19.0 | 14.8-16.6 |
| Cr | 3 | 4 | 3 | <3 | 3.0-3.6 | 3.0-3.4 | 4.0-4.1 |
| Rb | 141 | 66 | 109 | 202 | 106-124 | 81-132 | 119-135 |
| Sr | 494 | 328 | 355 | 322 | 503-739 | 515-528 | 382-412 |
| Pb | 10 | 11 | 9 | 14 | | | |
| Ba | 1020 | 127 | 270 | 683 | 727-1090 | 1030-1060 | 913-916 |
| Zr | 475 | 547 | 565 | 605 | 304-506 | 475-536 | 717-771 |
| Hf | 13.6 | n.d | 15.4 | 17.2 | 8.1-11.2 | 10.9-11.9 | 16.5-18.1 |
| Nb | 163 | 133 | 128 | 132 | | | |
| Ta | 6.0 | n.d | 7.1 | 7.6 | 3.7-5.2 | 5.1-5.4 | 6.8-8.0 |
| Y | 79 | 87 | 86 | 87 | 48-68 | 61-86 | 67-76 |
| Th | 9 | 10 | 13 | 19 | 5.3-7.9 | 6.9-16.8 | 13.7-21.8 |
| U | n.d. | n.d | n.d | n.d | n.d | 2.8 | 4.9-5.2 |
| Cs | 6.1 | n.d. | 6.2 | 4.0 | 3.9-5.2 | 1.8-4.5 | 2.2-6.4 |
| La | 100 | 54 | 68 | 74 | 61-100 | 94-102 | 101-111 |
| Ce | 232 | 150 | 186 | 174 | 137-215 | 203-224 | 226-235 |
| Nd | 115 | 92 | 102 | 91 | 78-116 | 109-117 | 112-116 |
| Sm | 20 | n.d. | 20 | 19 | 12.5-17.8 | 18.2-19.8 | 18-18.1 |
| Eu | 5.8 | n.d. | 5.1 | 4 | 3.7-5.9 | 5.9-6.0 | 5.1-5.5 |
| Tb | 3.0 | n.d. | 3.2 | 3 | 1.92-2.63 | 2.58-2.94 | 2.58-2.70 |
| Yb | 8.1 | n.d. | 5.5 | 8.1 | 4.33-5.76 | 4.97-7.12 | 6.34-7.55 |
| Lu | 1.0 | n.d. | 1.2 | 1.2 | 0.61-0.73 | 0.71-0.87 | 0.83-0.94 |
| Zn | 17 | 99 | 94 | 91 | | | |
| Ni | 13 | 4 | 4 | 3 | | | |
| V | 193 | 135 | 141 | 112 | | | |
| Cr | 3 | 4 | 3 | <3 | | | |
| Ga | 25 | 27 | 28 | 27 | | | |
| Th/La | 0.09 | 0.19 | 0.19 | 0.26 | 0.07-0.08 | 0.07-0.16 | 0.14-0.20 |
| Th/Ta | 1.50 | - | 1.83 | 2.50 | 1.35-1.54 | 1.36-3.11 | 2.01-2.72 |

Analysed at the Geological Survey of Denmark and Greenland and the Geological Institute, University of Copenhagen (J.C. Baily) and Tracechem A/S, Copenhagen (R. Gwozdz).

[1)] from Morogan and Sørensen (1994), n.d. = not analysed

Table 6. Sr and Nd isotope data

| Sample | | Rb | Sr | $^{87}Rb/^{86}Sr$ | $^{87}Sr/^{86}Sr$ | +-2σ | Sm | Nd | $^{147}Sm/^{144}Nd$ | $^{143}Nd/^{144}Nd$ | +-2σ | $^{87}Sr/^{86}Sr$ |
|---|---|---|---|---|---|---|---|---|---|---|---|---|
| | | parts per million | | | | | parts per million | | | | | 272 Ma |
| *Basaltic trachyandesites* | | | | | | | | | | | | |
| 92061 | dyke (dark) | 125 | 781 | 0.4637 | 0.70610 | 0.000011 | 20.1 | 108 | 0.1138 | 0.512598 | 0.000007 | 0.704310 |
| 23279 | black | 25 | 133 | 0.5345 | 0.70751 | 0.000043 | 5.69 | 30.8 | 0.1124 | 0.512630 | 0.000009 | 0.705440 |
| 23289 | black | 118 | 412 | 0.8305 | 0.70786 | 0.000042 | 22.2 | 123 | 0.1098 | 0.512604 | 0.000006 | 0.704643 |
| 77219 | black | 136 | 536 | 0.7337 | 0.70716 | 0.000009 | 21.0 | 112 | 0.1144 | 0.512609 | 0.000010 | 0.704318 |
| 77192 | black | 80 | 527 | 0.4410 | 0.70629 | 0.000013 | 22.3 | 122 | 0.1117 | 0.512621 | 0.000010 | 0.704585 |
| 78312 | black | 138 | 384 | 1.0422 | 0.70839 | 0.000010 | 22.8 | 125 | 0.1111 | 0.512620 | 0.000005 | 0.704352 |
| 77232 | grey | 112 | 488 | 0.6616 | 0.70679 | 0.000056 | 22.3 | 121 | 0.1124 | 0.512618 | 0.000008 | 0.704225 |
| 77238 | grey | 124 | 507 | 0.7076 | 0.70702 | 0.000012 | 23.5 | 125 | 0.1145 | 0.512625 | 0.000007 | 0.704285 |
| 77241 | grey | 109 | 734 | 0.4283 | 0.70636 | 0.000087 | 15.4 | 82.0 | 0.1144 | 0.512526 | 0.000007 | 0.704701 |
| 77191 | grey | 124 | 505 | 0.7111 | 0.70708 | 0.000024 | 22.4 | 121.9 | 0.1118 | 0.512601 | 0.000006 | 0.704330 |
| Emulsified enclaves | | | | | | | | | | | | |
| HS 101252* | black, homog | 141 | 494 | 0.8260 | 0.70744 | 0.000023 | 20.0 | 104 | 0.11591 | 0.512604 | 0.000005 | 0.704240 |
| HS 101253a* | black emulsified | 109 | 355 | 0.8886 | 0.70784 | 0.000017 | 19.3 | 95.1 | 0.12274 | 0.512615 | 0.000005 | 0.704401 |
| HS 101253b* | total mixture | 202 | 322 | 1.8155 | 0.71146 | 0.000023 | 17.7 | 89.3 | 0.11982 | 0.512611 | 0.000004 | 0.704435 |
| HS 101253c* | single black globule | 66 | 328 | 0.5823 | 0.706751 | 0.000020 | 17.9 | 91.4 | 0.11864 | 0.512621 | 0.000006 | 0.704497 |
| Granites | | | | | | | | | | | | |
| 86044 | Medium-grained granite | 82 | 24 | 9.817 | 0.74226 | 0.000009 | 7.78 | 44.4 | 0.1068 | 0.512622 | 0.000010 | 0.704271 |
| 86069 | Fine-grained granite | 236 | 18 | 38.61 | 0.85290 | 0.000022 | 16.6 | 72.0 | 0.1408 | 0.512676 | 0.000010 | 0.703461 |
| 86045 | Ekerite | 261 | 4 | 208.1 | 1.51013 | 0.000029 | 18.1 | 70.8 | 0.1559 | 0.512673 | 0.000007 | 0.704688 |
| 86057 | Ekerite | 272 | 37 | 21.32 | 0.78366 | 0.000027 | 10.9 | 45.3 | 0.1466 | 0.512688 | 0.000009 | 0.701161 |
| 86035 | Fine-grained granite | 265 | 17 | 46.33 | 0.88289 | 0.000012 | 19.1 | 102 | 0.1137 | 0.512608 | 0.000009 | 0.703590 |
| 86018 | Fine-grained granite | 88 | 3 | 97.89 | 1.07818 | 0.000029 | 1.30 | 6.29 | 0.1264 | 0.512638 | 0.000014 | 0.699342 |

*: Analysed at the Geological Institute, Copenhagen University, Denmark (Robert Frei, analyst).

for the granites, but are within its large error envelope (Fig. 6b). Time-corrected $^{87}Sr/^{86}Sr$ and $\varepsilon_{Nd}$ at 272 Ma are compared to the ranges of extrusive and intrusive rocks from the Oslo Region in Fig. 7 (for sources of reference data, see figure caption). The black and emulsified trachyandesites show uniform initial Nd isotope composition ($\varepsilon_{Nd}$ = +2.2 ±0.5), but show variations in $^{87}Sr/^{86}Sr_{272Ma}$ in excess of analytical error (Fig. 7, expanded detail), defining a sub-horizontal trend in the diagram towards increasing $^{87}Sr/^{86}Sr_{272Ma}$. A disrupted basic dyke, and three of the four samples of grey trachyandesite, have Sr and Nd isotopic compositions at 272 Ma indistinguishable from the low-$^{87}Sr/^{86}Sr$ end of the trend of the black and emulsified trachyandesites, whereas the fourth sample of grey trachyandesite (77241) falls off towards significantly lower epsilon Nd and slightly increased $^{87}Sr/^{86}Sr_{270Ma}$, suggesting a separate mixing trend.

The granitic samples show $\varepsilon_{Nd}$ at 272 Ma in the range +2.1 to + 2.8, overlapping with the main group of basaltic trachyandesite. The time-corrected $^{87}Sr/^{86}Sr$ ratios have such large uncertainties (above), that only two of the six granite samples analysed (Table 6) plot within the scale of Fig. 7.

## Discussion

Based on petrography, mineral chemistry and major and trace element chemistry, Morogan & Sørensen (1994) proposed that the trachyandesitic members of the net-veined complexes are hybrid rocks formed by mixing of basaltic and trachytic magmas in the deep crust. These hybrid magmas were injected into a partly consolidated granitic/syenitic magma chamber which led to additional hybridization.

The occurrence of edenite in the homogeneous trachyandesite and in the trachyandesite hosting the granite globules indicates that the trachyandesitic magma was under influence of a granitic component during crystallization. This inference comes from the fact that edenitic compositions are similar to the amphiboles formed close to granite described by Morogan & Sørensen (1994), and are considered to reflect P-T-X conditions of crystallization controlled by the granitic magma.

The low-Ca augite of the trachyandesite could be explained by rapid cooling conditions; in this case, possibly due to small drops of a hotter basic magma quickly emulsified within a cooler granitic magma. The emulsified type of enclaves may be explained by the fragmentation of pillows of basic magma into smaller globules which were mixed with the host acidic magma (cf. Gourgaud 1991). The chemical data of Table 5 show, however, that the basic globules of the emulsified rock (101253a, c) are chemically distinct from the screen of homogeneous trachyandesite (101252) and also from the mixed rocks (101253b). When compared with the homogeneous trachyandesite, the emulsified bodies have higher contents of $SiO_2$, $Na_2O$, Zr and Y, and lower con-

| +-2σ | $\varepsilon_{Nd}$ 272 Ma | +-2σ |
|---|---|---|
| 0.000011 | 2.10 | 0.1 |
| 0.000043 | 2.77 | 0.2 |
| 0.000042 | 2.35 | 0.1 |
| 0.000009 | 2.28 | 0.2 |
| 0.000013 | 2.63 | 0.2 |
| 0.000010 | 2.61 | 0.1 |
| 0.000056 | 2.53 | 0.2 |
| 0.000012 | 2.60 | 0.1 |
| 0.000087 | 0.66 | 0.1 |
| 0.000024 | 2.23 | 0.1 |
| 0.000023 | 2.14 | 0.1 |
| 0.000017 | 2.12 | 0.1 |
| 0.000023 | 2.13 | 0.1 |
| 0.000020 | 2.38 | 0.1 |
| 0.000009 | 2.81 | 0.2 |
| 0.000022 | 2.67 | 0.2 |
| 0.000029 | 2.10 | 0.1 |
| 0.000027 | 2.71 | 0.2 |
| 0.000012 | 2.30 | 0.2 |
| 0.000029 | 2.43 | 0.3 |

tents of $TiO_2$, MgO, CaO, $K_2O$, $P_2O_5$, l.o.i., Rb, Sr, Ba and LREE, contents which fall outside the range of the earlier analysed trachyandesites of Table 5. When compared with the mixed rocks, the black globules have higher $TiO_2$, $Al_2O_3$, MgO, CaO, $Na_2O$, $P_2O_5$, l.o.i., Sc and Sr, and lower $SiO_2$, FeO, $K_2O$, Rb, Ba, Zr, Hf and Th. This indicates that a combination of mechanical and chemical mixing has been involved in the formation of the emulsified rock and that the trachyandesitic magma was chemically inhomogeneous at the time of intrusion.

Morogan and Sørensen (1994) used the Th/La and Th/Ta ratios of the Mykle net-veined rocks together with ratios of some other rocks from the Oslo Rift, in order to depict mixing between mantle-derived magmas and material of lower and/or upper crustal origin. The Th/La and Th/Ta ratios of the homogeneous trachyandesite (Table 5) are similar to those of the grey trachyandesite from Mykle, which plotted on a mixing line between mantle and lower crustal materials (Morogan & Sørensen 1994, fig. 18). The much higher ratios exhibited by the emulsified trachyandesite samples (Table 5) indicate mixing with an upper crustal material, i.e., in a granite/syenite magma chamber.

All but two of the samples of basaltic trachyandesite analysed by Morogan & Sørensen (1994) fall within the ranges of $^{87}Sr/^{86}Sr$ and $\varepsilon_{Nd}$ at 272 Ma of basaltic lavas of the Vestfold and Jeløya regions, and of larvikite from the Larvik pluton (Fig. 7). On the other hand, the composition of the basaltic trachyandesite is distinctly different from that of the Skien basalts. The trachyandesitic component in the net-veined complexes at lake Mykle may therefore be genetically related to the moderately alkaline lavas of the Vestfold-Jeløy area, and/or to larvikite, or it may have been derived from a similar mantle source. The much more alkaline and silica-undersaturated magmas of the Skien basalts, and their mantle source, cannot have contributed to the petrogenesis of the trachyandesite in the net-veined complexes.

The tendency of a sub-horizontal trend towards increasing initial $^{87}Sr/^{86}Sr$ in the black and emulsified trachyandesites (Fig. 7, expanded detail) indicates that the black trachyandesite (including the black components in the emulsified rock) was initially heterogeneous in strontium isotopes, most likely because of selective introduction of Sr with elevated $^{87}Sr/^{86}Sr$ by an aqueous fluid prior to or during emplacement. The one outlying sample of grey trachyandesite, on the other hand, may suggest a different mixing trend, most likely attributable to bulk contamination with material with $\varepsilon_{Nd} = 0$ and $^{87}Sr/^{86}Sr_{272Ma} = 0.7045$. Precambrian basement rocks (Andersen & Knudsen 2000) or crustally contaminated, Late Paleozoic granitic or syenitic rocks may be suitable contaminants (Fig. 7).

The ellipsoidal bodies of granite enclosed in massive trachyandesite present a special problem. The granite is coarse-grained and cannot be distinguished from the main body of granite enclosing the net-veined complexes. The enclosing trachyandesite is enriched in biotite up to about 2 cm from the contact with the granite. The granite bodies have rounded ellipsoidal shapes and two such round bodies may coalesce. The following explanations may be proposed for the origin of the granite bodies.

(1) The granite globules represent lumps of partly consolidated granite engulfed by the intruding basic magma. Crystallization of the granite was extended by inclusion in the hotter basic magma, which explains the large grain size of the granite and the coalescence of two such partly liquid globules. Fluids expelled from the crystallizing granitic melt may explain the formation of biotite at the expense of the amphibole of the enclosing trachyandesite. A variation of this explanation is that fragments of already consolidated granite were caught by the invading hot basic magma and were softened and perhaps partly melted in their marginal parts, which explains the rounded shapes. Reactions with volatiles released from the partly molten granite fragments were the cause of the formation of biotite in the host basic rock.

(2) The ellipsoidal bodies of granite are cross sections of pipes of granite invading the trachyandesite.

The lack of longitudinal sections of such pipes suggests that explanation (2) is unlikely, and explanation (1) is therefore preferred. Thus, the emulsified rocks show mingling of droplets of basic magma with granitic magma, whereas the granite ellipsoids in trachyandesite indicate the opposite relationship.

## Conclusions

The new field and petrographical observations presented here, and the major and trace element data, support a petrogenetic model for the generation of net-veined complexes consisting of trachyandesitic and granitic/syenitic components as proposed by Morogan & Sørensen (1994). The model involves a first stage of mixing of magmas at depth, followed by in-situ mingling of mafic and felsic magmas when trachyandesitic melts were injected into a solidifying granitic or syenitic magma chamber. Sr and Nd isotope data add further support to this model, and indicate that the trachyandesitic component in the net-veined complexes is either genetically related to larvikite or basaltic lavas of the Vestfold-Jeløya type, or derived from a similar mantle source. Variations in initial strontium isotope compositions in the trachyandesite, which are uncorrelated with neodymium isotopes, are due to selective introduction of more radiogenic strontium by a fluid phase before or during

emplacement of the trachyandesitic melt. Ellipsoidal bodies of granite contained in the trachyandesite represent blocks of granite or pockets of partly solidified granitic melt engulfed in the mafic component during the mingling process.

*Acknowledgements*

The field and laboratory investigations of HS and VM were supported by the Geological Survey of Norway, the Danish Natural Science Research Council and the Carlsberg Foundation. We are grateful for analyses and analytical assistance provided by Toril Enger (Mineralogical-Geological Museum, University of Oslo), the Geological Survey of Denmark and Greenland, John C. Bailey and Robert Frei (Geological Institute, Copenhagen University) and R. Gwozdz (Tracechem A/S, Copenhagen). Britta Munch and Ole Bang Berthelsen assisted with the preparation of illustrations. Constructive criticism from the reviewers Calvin Barnes and Tore Prestvik, is gratefully acknowledged.

## References

Andersen, T. & Knudsen, T.-L. 2000: Crustal contaminants in the Permian Oslo Rift, South Norway: constraints from Precambrian geochemistry. *Lithos 53*, 247–264.

Andersen, T., Andresen, A. & Sylvester, A.G. 2001: Nature and distribution of deep crustal reseervoirs in the southwestern part of the Baltic Shield: evidence from Nd, Sr and Pb isotope data on late Sveconorwegian granites. *Journal of the Geological Society, London 158*, 253-267.

Andersen, T., Frei, R., Sørensen, H. & Westphal, N. L. 2004: Porphyritic syenite at Lake Mykle, the Oslo Rift – a possible derivative of larvikite. *Norges geologiske undersøkelse Bulletin 432*, 23–28.

Bonin, B. & Sørensen, H. 2003: The granites of the Mykle region in the southern part of the Oslo igneous province, Norway. *Norges geologiske undersøkelse Bulletin 441*, 17–24.

Boynton, V.W. 1984: Cosmochemistry of the rare earth elements. Meteorite studies. In: *Rare Earth Element Geochemistry, Developments in Geochemistry 2*, Elsevier, Amsterdam, 63-114.

Dunworth, E.A., Neumann, E.-R. & Rosenbaum, J.M. 2001: The Skien lavas, Oslo Rift: petrological disequilibrium and geochemical evolution. *Journal of Petrology 140*, 701719.

Gourgaud, A. 1991: Comagmatic enclaves in lavas from the Mont-Dore composite volcano, Massif Central, France. In: Didier, J. & Barbarin, B. (eds.): *Enclaves and Granite Petrology*. Elsevier, Amsterdam, 221–233.

Leake, B. E., Woolley A.R., Arps, C.E.S., Birch, W.D., Gilbert, M.C., Grice, J.D., Hawthorne, F.C., Kato, A., Kisch, H.J., Krivovichev, V.G., Linthout, K., Laird, J., Mandarino, J.A., Maresch, W.V., Nickel, E.H., Rock, N.M.S., Schumacher, J.C., Smith, D.C., Stephenson, N.C.N., Ungaretti, L., Whittaker, E.J.W. & Guo, Y.Z. 1997: Nomenclature of amphiboles: report of the Subcommittee on Amphiboles of the International Mineralogical Association, Commission on New Mineral and Mineral Names. *Canadian Mineralogist 35*, 219–246.

Ludwig, K.R. 2003 Isoplot 3.00. A geochronological toolkit for Microsoft Excel. *Berkeley Geochronology Centre Special Publication No. 4.*

Morimoto, N., Fabries, J., Ferguson, A.K., Ginzburg, I.V., Ross, M., Seifert, F.A., Zussman, J., Aoki, K. & Gottardi, G. 1988: Nomenclature of pyroxenes. Subcommittee on Pyroxenes, Commission on New Mineral and Mineral Names. International Mineralogical Association. *Bulletin Minéralogique 111*, 535–555.

Morogan, V. & Sørensen, H. 1994: Net-veined complexes in the Oslo rift, southeast Norway. *Lithos 32*, 21–45.

Neumann, E.-R., Tilton, G.R. & Tuen, E. 1988: Sr, Nd and Pb isotope geochemistry of the Oslo Rift igneous province, southeast Norway. *Geochimica Cosmochimica Acta 52*, 1997-2002.

Neumann, E.-R., Dunworth, E.A., Sundvoll, B.A. & Tollefsrud, J.I. 2002: B1 basaltic lavas in Vestfold-Jeløya area, central Oslo rift: derivation from initial melts formed by progressive partial melting of an enriched mantle source. *Lithos 61*, 21-53.

Rasmussen, E., Neumann, E.-R., Andersen, T., Sundvoll, B., Fjerdingstad, V. & Stabel. A. 1988: Petrogenetic processes associated with intermediate and silicic magmatism in the Oslo Rift, southeast Norway. *Mineralogical Magazine 52*, 293-307.

Sundvoll, B. & Larsen, B.T. 1990: Rb-Sr systematics in the Oslo rift magmatic rocks. *Norges geologiske undersøkelse Bulletin 418*, 27-46.

Trønnes, R.G. & Brandon, A.D. 1992: Mildly peraluminous high-silica granites in a continental rift: the Drammen and Finnemarka batholiths, Oslo Rift, Norway. *Contributions to Mineralogy and Petrology 109*, 275-294.